Analyzing power and cross section distributions of the $^{12}C(p,p\alpha)^{8}Be$ cluster knockout reaction at an incident energy of 100 MeV

J. Mabiala,[1,2,*] A. A. Cowley,[1,2,†] S. V. Förtsch,[2] E. Z. Buthelezi,[2] R. Neveling,[2] F. D. Smit,[2] G. F. Steyn,[2] and J. J. Van Zyl[1]

[1]*Department of Physics, Stellenbosch University, Private Bag X1, Matieland 7602, South Africa*

[2]*iThemba Laboratory for Accelerator Based Sciences, Somerset West 7129, South Africa*

(Received 24 March 2009; published 21 May 2009)

The $(p,p\alpha)$ reaction on ^{12}C was investigated experimentally using polarized incident protons of 100 MeV. The scattered proton and α particle, from the knockout reaction, were detected in coincidence. Coincident data, which were obtained at ten quasifree angle pairs for proton angles ranging from 25° to 110°, were analyzed in terms of the distorted-wave impulse approximation (DWIA). Calculated energy-sharing cross section and analyzing power distributions reproduce the data reasonably well, indicating that a quasifree knockout mechanism dominates the reaction. Since measurements of analyzing powers were made, spin-orbit distortions were included in the DWIA calculations. The effects of this were found to be very small near zero recoil momentum and did not destroy the validity of the factorization approximation where the two-body p-α cross section enters as a multiplicative factor in the three-body $(p,p\alpha)$ cross section expression. Spectroscopic factors derived from the data are consistent with theoretical predictions. Analyzing power data also follow the trend of free p-^{4}He scattering data, and comparisons with DWIA predictions are in reasonable agreement. Because the two-body interaction response between the projectile and the α cluster was found to resemble the scattering of protons from a free α particle to a remarkable degree, the present results would strongly imply the existence of preformed α clusters in ^{12}C.

DOI: 10.1103/PhysRevC.79.054612 PACS number(s): 25.40.−h, 24.70.+s, 21.60.Gx, 27.20.+n

I. INTRODUCTION

Knockout reactions offer a direct and convenient technique for investigating the clustering of atomic nuclei in their ground state and thus have in the past greatly contributed to our understanding of the α-cluster structure of the nuclear medium. Distorted-wave impulse approximation (DWIA) calculations [1,2], when compared with experimental coincidence cross section distributions from the $(p,p\alpha)$ reaction, suggest that the reaction mechanism is reasonably simple. For example, for the light nuclei ^{6}Li, ^{7}Li, ^{9}Be, and ^{12}C, Roos *et al.* [3] found that experimental $(p,p\alpha)$ energy-sharing cross section distributions at an incident energy of 100 MeV are in reasonable agreement with theoretical expectation. Also, spectroscopic factors extracted from the data, which are related to cluster occupation probabilities, appear to be consistent with shell model estimates. Another indication of a simple reaction mechanism is the factorization of the cross section into a form in which the projectile-cluster interaction appears separately from the cluster-core structure function. This seems to be appropriate for very light target nuclei [3], but perhaps to a lesser extent for the ^{12}C nucleus. Of course, as discussed by Chant and Roos [2], factorization of the coincidence cross section is only possible if fairly drastic approximations, such as neglecting spin-orbit interactions in the distorting potentials, are made to the full DWIA theory. Nevertheless, the observed experimental factorization of the cross section suggests that it is reasonable to infer that the heavy core of the cluster system acts merely as spectator to the collision between the projectile and the cluster, without transfer of momentum to it from the two-body collision.

In another $(p,p\alpha)$ study, also at an incident energy of 100 MeV, on the target nuclei ^{16}O, ^{20}Ne, ^{24}Mg, ^{28}Si, ^{32}S, ^{40}Ca, ^{48}Ti, ^{54}Fe, and ^{66}Zn, Carey *et al.* [4] reported similar agreement between experimental energy-sharing cross section distributions and predictions of the factorized DWIA theory. Over this large mass range of target nuclei, spectroscopic factors were found to display the same trend as results from pickup reactions.

More rigorous investigations of the DWIA description of $(p,p\alpha)$ reactions become possible with polarized proton beams. For example, as an extreme test of the factorization approximation, measurements of $(p,p\alpha)$ analyzing power distributions can be compared directly against those measured in free p-^{4}He elastic scattering [5]. The ability to reproduce experimental analyzing powers clearly provides a better indication of the reaction dynamics, which consequently lends credibility to conclusions drawn about the cluster structure of the studied nuclei [6]. Wang *et al.* [5] found satisfactory agreement between the energy-sharing analyzing power distribution and DWIA calculations for the $^{9}Be(p,p\alpha)$ reaction at 150 MeV. In the same way, Yoshimura *et al.* [6] confirmed the results for the $(p,p\alpha)$ reaction at 296 MeV for the targets ^{6}Li, ^{7}Li, and ^{9}Be. This indicates that the reaction is largely governed by a quasifree process. The differences between the experimental analyzing power and DWIA calculations for the $^{12}C(p,p\alpha)^{8}Be$ reaction at 296 MeV [6] were interpreted as due to significant contributions from processes other than quasifree scattering. However, one should keep in mind that conclusions about the reaction mechanism were complicated because the knockouts to the ground state and the first excited state of the final nucleus ^{8}Be were not experimentally resolved.

*mabiala@sun.ac.za
†aac@sun.ac.za

The first investigation of the analyzing power on a target as heavy as ^{40}Ca [7], as a test of the α-cluster knockout reaction, failed to confirm the standard simple interpretation applicable to lighter targets. The experimental analyzing power distribution could not be reproduced by DWIA calculations. Consequently, the present investigation focuses on the knockout reaction on ^{12}C in an experiment in which the ground state of the final nucleus is resolved. A nucleus that is so much lighter than ^{40}Ca should perhaps be less sensitive to ingredients of the DWIA. Another advantage is that ^{12}C has been studied more extensively than ^{40}Ca in knockout experiments [3,8,9]. A thorough understanding of the analyzing power distribution for $^{12}C(p,p\alpha)^{8}$Be could provide guidance for obtaining insight into the issues affecting ^{40}Ca.

Recently we presented a detailed study [10] of the analyzing power distribution for $^{12}C(p,p\alpha)^{8}$Be(g.s.). For the target nucleus ^{12}C, a single cluster-core angular momentum value contributes to the knockout yield, which simplifies the theoretical interpretation and consequently enhances the credibility of the findings. We found that the DWIA prediction of the analyzing power distribution followed the trend of the experimental values only qualitatively. However, this lack of detailed agreement could be due to inappropriate optical model parameters for the $p + {}^{4}$He system, which similarly failed to reproduce the elastic scattering analyzing power angular distribution at the same incident energy.

Some of the experimental data presented in this work were presented in our previous paper [10]. However, we now provide additional results from the same experiment and perform a more extensive DWIA theoretical investigation of analyzing power and cross section distributions. Also, as we had proposed in Ref. [10], we recalculated the DWIA analyzing power angular distribution [at zero recoil momentum of the ^{8}Be residual nucleus in the $^{12}C(p,p\alpha)^{8}$Be reaction] with an improved set of optical model parameters adjusted to reproduce the experimental observables from $p + {}^{4}$He elastic scattering more accurately. Apart from additional insight into details of the agreement between DWIA theory and experimental distributions, the present results lend further support to the validity of conclusions from our previous work.

II. THE EXPERIMENT

A. Experimental setup and procedure

A 101 ± 0.5 MeV proton beam, polarized to approximately 80% and with beam intensities of up to 100 nA, was delivered by the separated-sector cyclotron facility of iThemba Laboratory for Accelerator Based Sciences to irradiate a self-supporting carbon foil of 2.2 mg cm^{-2} thickness inside a 1.5 m diameter scattering chamber. The beam polarization was monitored regularly with a polarimeter upstream from the scattering chamber, which consisted of a CH_2 target and two NaI(Tl) detectors. Beam polarization was switched from up to down at 10 s intervals to minimize systematic errors in the measurements. The difference in the polarization between the two orientations was always less than 15%.

The scattered protons and α particles were detected in coincidence with two detector telescopes, mounted coplanar on opposite sides of the beam. The telescope for proton detection consisted of a 1 mm thick Si surface-barrier transmission detector followed by a 7.6 cm diameter by 5.1 cm thick NaI(Tl) crystal-phototube assembly. A 100 μm thick surface-barrier transmission detector, followed by two 2 mm thick surface-barrier transmission detectors, made up the telescope used for α-particle detection. Behind this telescope was a 7.6 cm diameter by 5.1 cm thick NaI(Tl) crystal-phototube assembly, which acted as a veto for energetic protons. The subtended solid angles were 5.26 msr for the proton telescope and 1.31 msr for the α-particle telescope.

Energy calibrations of the four Si detectors were carried out with α particles obtained from ^{228}Th radioactive sources. Protons scattered from ^{12}C provided the means for energy calibration of the NaI(Tl) detector in the proton telescope. Possible gain drifts in the photomultiplier tubes of the NaI detectors were corrected by monitoring a light-emitting diode (LED) pulser system. The LED was triggered at a rate proportional to the beam current, and these pulses were also used to correct for electronic dead time. Charged-particle identification was achieved through standard ΔE-E techniques. However, for the three smallest proton angles, most of the α particles that satisfy the quasifree condition were stopped in the ΔE detector, therefore a ΔE-E coincidence for the α telescope did not occur for those events. Consequently, the hardware coincidence requirement for α-particle identification was turned off in the electronic setup at those angles. Q-value considerations then allowed the analysis of events without valid ΔE-$E\alpha$-particle coincidences.

The electronic system used to process linear and fast timing signals was composed of standard NIM and CAMAC units. A VAX computer system was used for online sorting and offline replay of data. All data were written event-by-event to hard disks for subsequent offline replay.

B. Experimental data

Measurements were made at ten coplanar angle pairs $(\theta_p, \theta_\alpha)$ ranging from $(25^\circ, -68.8^\circ)$ to $(110^\circ, -26.6^\circ)$; see Table I. These angles were chosen to permit zero recoil

TABLE I. Angle pairs θ_p/θ_α, two-body center-of-mass scattering angle $\theta^{\text{c.m.}}_{p\text{-}\alpha}$, measured cross section $d^3\sigma/d\Omega_p\, d\Omega_\alpha\, dE_p$, and analyzing power A_y values at the quasifree peak.

θ_p/θ_α (deg)	$\theta^{\text{c.m.}}_{p-\alpha}$ (deg)	$d^3\sigma/d\Omega_p\, d\Omega_\alpha\, dE_p$ (mb sr^{-2} MeV^{-1})	A_y
25.0/−68.8	31.9	$(1.35 \pm 0.054) \times 10^{-1}$	0.39 ± 0.03
30.0 /−66.6	38.2	$(1.52 \pm 0.046) \times 10^{-1}$	0.43 ± 0.04
37.0/−63.1	46.8	$(1.36 \pm 0.073) \times 10^{-1}$	0.24 ± 0.04
52.0/−55.1	64.9	$(1.66 \pm 0.741) \times 10^{-2}$	-0.11 ± 0.06
60.0/−50.9	74.1	$(1.82 \pm 0.106) \times 10^{-2}$	-0.39 ± 0.09
70.0/−45.6	85.3	$(1.70 \pm 0.051) \times 10^{-2}$	-0.26 ± 0.04
80.0/−40.5	96.0	$(0.89 \pm 0.035) \times 10^{-2}$	-0.55 ± 0.06
90.0/−35.7	106.2	$(4.06 \pm 0.200) \times 10^{-3}$	-0.41 ± 0.07
100.0/−31.0	115.9	$(3.15 \pm 0.311) \times 10^{-3}$	-0.16 ± 0.14
110.0/−26.6	125.2	$(4.31 \pm 0.440) \times 10^{-4}$	0.22 ± 0.14

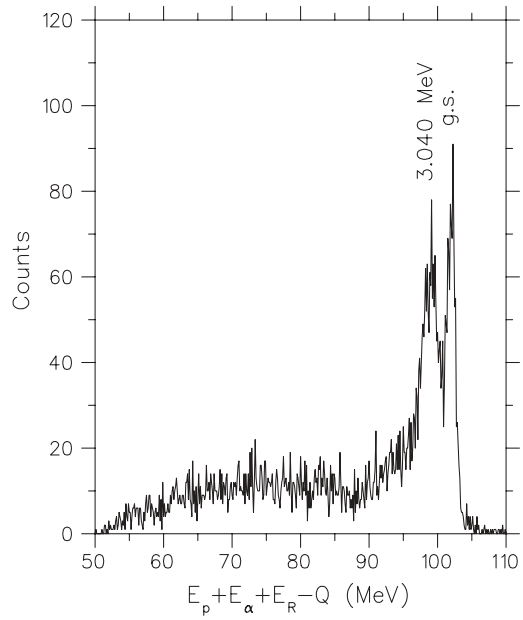

FIG. 1. Typical binding energy spectrum obtained from a projection of the data onto the total energy axis. The ground state and first excited state of the residual nucleus ^{8}Be are clearly resolved.

momentum of the undetected nucleus ^{8}Be. For each angle pair, a two-dimensional coincidence spectrum of total energy ($E_p + E_\alpha + E_R - Q$) versus proton energy (E_p) was generated. The subscripts p,α, and R refer, respectively, to proton, alpha, and recoil particle; Q is the ground-state Q-value of the reaction. The quantity E_R was calculated from the measured energies of the outgoing particles and given reaction parameters such as particle mass, incident energy, and angle of detection. To clearly identify the extent of the quasifree knockout locus, the data were projected onto the total energy axis, resulting in a binding energy spectrum. A typical binding energy spectrum, with a missing-mass resolution of approximately 1.5 MeV and a total energy scale within the experimental uncertainty of 2%, is presented in Fig. 1. Based on a gate on the binding energy spectrum, events associated with knockout to the ground state of the residual nucleus were selected. These events were then projected onto the proton energy axis to extract an energy-sharing distribution.

The experimental analyzing power is calculated as

$$A_y = \frac{C^{\uparrow} - C^{\downarrow}}{p^{\downarrow}C^{\uparrow} + p^{\uparrow}C^{\downarrow}}, \tag{1}$$

where $C^{\uparrow(\downarrow)}$ represents the quasifree knockout yield for upward (downward) polarized beam, and $p^{\uparrow(\downarrow)}$ is the beam polarization for the spin-up (spin-down) data. The (p, $p\alpha$) cross sections and analyzing powers at different quasifree angle pairs are displayed in Figs. 2 and 3. The errors on the data points are statistical errors only. The systematic errors in the cross

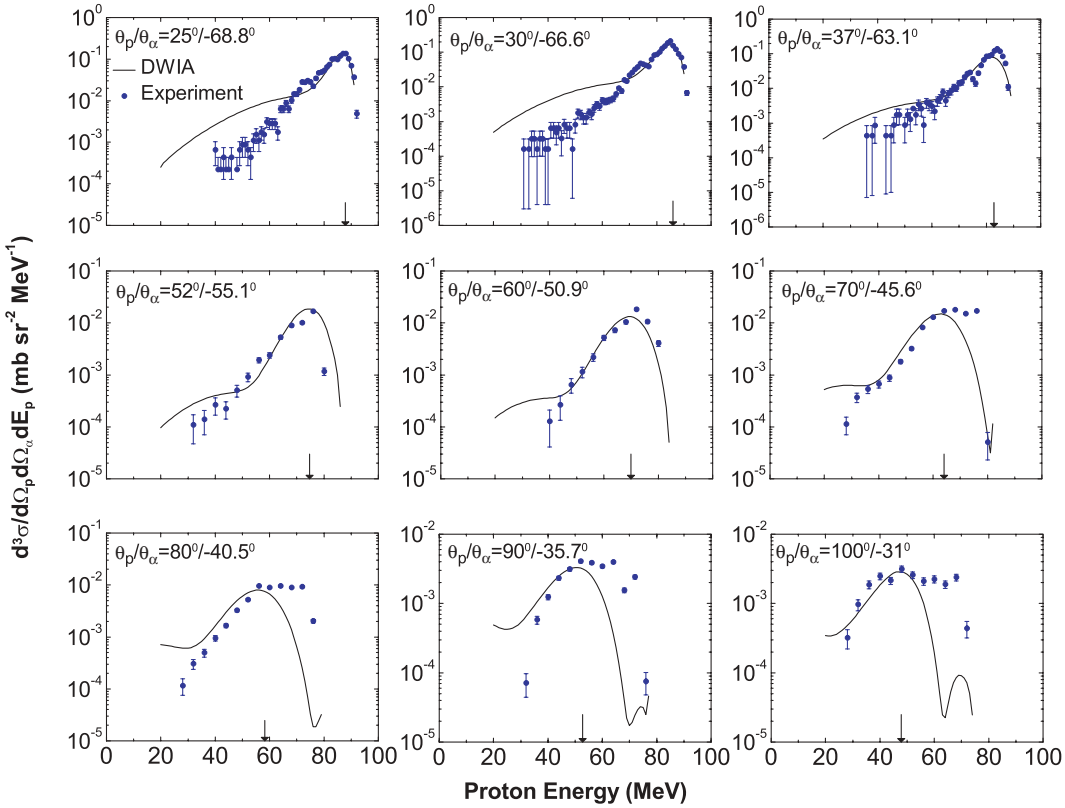

FIG. 2. (Color online) Cross section distributions projected onto the proton energy axis for the reaction ^{12}C(p,$p\alpha$)^{8}Be(g.s.). Statistical error bars on the experimental values are indicated. The curves represent results of DWIA calculations with the distorting potentials of set I in Table II. Spectroscopic factors for the theoretical cross section distributions are listed in Table III. The proton energy that corresponds to zero recoil momentum of the residual nucleus is indicated with an arrow for each angle pair.

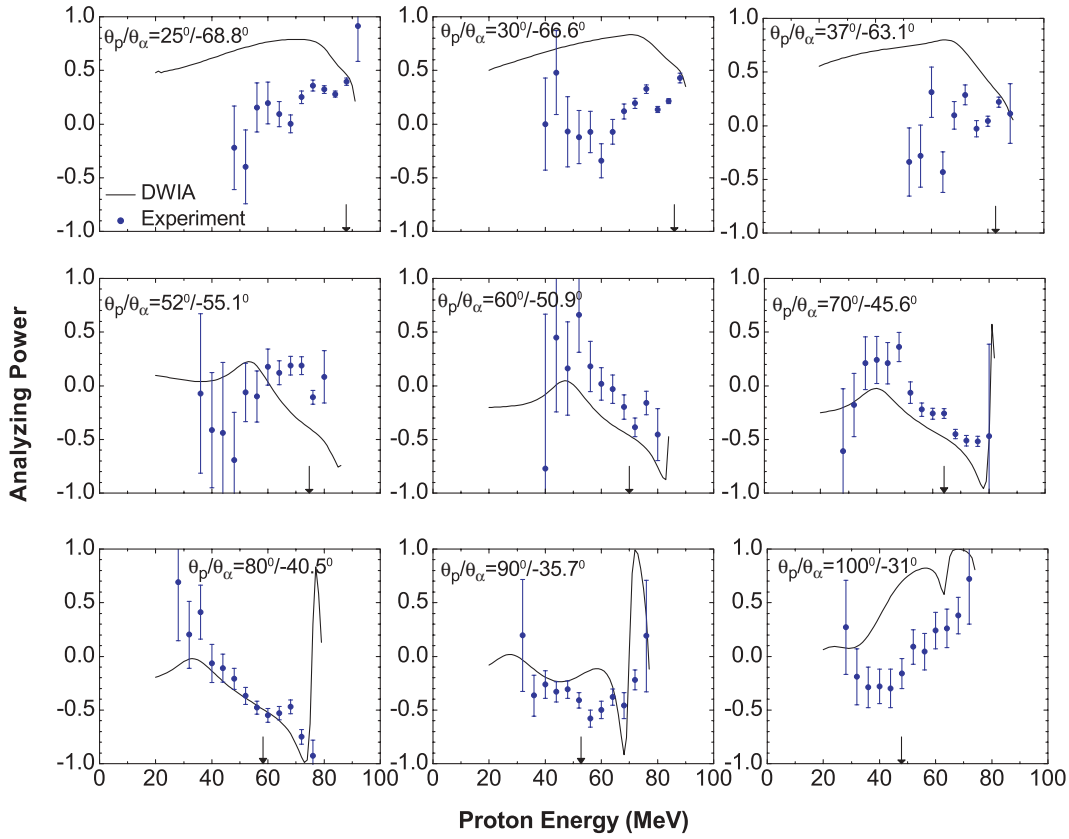

FIG. 3. (Color online) Same as Fig. 2, but for the analyzing power distributions.

sections are estimated to be less than 10%, while the accuracy in determining the analyzing power data, which are ratios of cross sections, is dominated by statistical errors. In both these figures, the proton energy that corresponds to zero recoil momentum of the residual nucleus is indicated with an arrow for each angle pair.

The energy-sharing cross sections in Fig. 2 are characterized by a smooth broad distribution reaching a maximum near the energy corresponding to zero recoil momentum for the residual nucleus, thus clearly showing the dominance of a quasifree α-cluster knockout. However, at proton angles at and above 70° we find that the cross section does not drop away at proton energies beyond the zero recoil position, as would be expected. As pointed out by Roos *et al.* [3], this effect could be due to the excitation of the ^{12}C target nucleus with subsequent α-particle sequential decay. However, the onset of these events appear to be appreciable only at higher proton energy than the expected maximum of the quasifree cross section. The presence of sequential events could in principle affect the extraction of spectroscopic factors, but we do not observe a systematic trend as would be expected. Hence it is unlikely that conclusions from our experimental cross section distributions were adversely affected by the decay events.

III. THEORETICAL CALCULATIONS

The theoretical analysis of the data was performed using a DWIA formalism, developed by Chant and Roos [2], that includes a spin-orbit interaction in the distorted waves in order to properly treat spin observables such as analyzing power. The calculations, performed with this model, are based on the general expression for a knockout reaction $A(a, cd)B$, where $A = B + b$, and c is the quasifree-scattered projectile a after an interaction with the bound particle b, which is emitted from the target nucleus as particle d. Applying the theory to the $(p, p\alpha)$ reaction implies $b = d$, which is a spinless particle, and $a = c$. The differential cross section for such a reaction is reduced to the expression

$$\frac{d^3\sigma}{d\Omega_c\, d\Omega_d\, dE_c} = S_\alpha K \sum_{\rho'_c L\Lambda} \left| \sum_{\rho_a\sigma_a\sigma_c\sigma'_c} D^{s_a}_{\rho_a\rho'_a}(R_{ap}) D^{s^*_a}_{\sigma_c\sigma'_c} \times (R_{ac}) T^{L\Lambda}_{\sigma_a\sigma'_c\rho_a\rho'_c} \langle\sigma_c|t|\sigma_a\rangle \right|^2, \quad (2)$$

where S_α is a spectroscopic factor, K is a kinematic factor, D are rotation matrices, and $\langle\sigma_c|t|\sigma_a\rangle$ denotes the matrix element of the two-body p-α transition operator.

The quantity $T^{L\Lambda}_{\sigma_a\sigma'_c\rho_a\rho'_c}$ is expressed as

$$T^{L\Lambda}_{\sigma_a\sigma'_c\rho_a\rho'_c} = (2L+1)^{-1/2} \times \int \chi^{(-)*}_{\sigma'_c\rho'_c}(\mathbf{r}) \chi^{(-)*}_a(\mathbf{r}) \phi_{L\Lambda}(r) \chi^{(+)}_{\sigma'_a\rho_a}(\gamma\mathbf{r})\, d\mathbf{r}, \quad (3)$$

where $\gamma = A/B$, χ represents the distorted waves for the incoming and outgoing particles, and $\phi_{L\Lambda}$ is the bound state wave function of the α cluster in the target nucleus, which represents the projection of the target wave function on the

product of α cluster and residual nucleus wave functions. More details of Eq. (2) and especially the definition of the notation used can be found elsewhere [1,2].

As was mentioned in the Introduction, when spin-orbit potentials are omitted in the distorted-wave calculations, the above cross section expression reduces to the so-called factorized form, in which the two-body $a + b \rightarrow c + d$ cross section, denoted by $|\langle\sigma_c|t|\sigma_a\rangle|^2$, enters as a multiplicative factor. Because particle b, bound in the target nucleus, is not on the energy-shell—i.e., two-body momentum and energy conservation are not satisfied due to the binding of the cluster b to the nucleus—the two-body cross section is a half-off-shell quantity. An additional approximation is therefore made by replacing this cross section with a nearby on-shell cross section. The energy at which this two-body interaction takes place can be chosen to be either the incident energy or the outgoing energy. The latter prescription is used in this work, in accordance with some earlier work (for example, Ref. [3]).

The computer code THREEDEE, written by Chant, was used to carry out the DWIA calculations [11]. The distorted waves and bound state wave function were generated from optical model potentials. The optical potential is defined as

$$U(r) = -\frac{V_R}{1+e^{X_R}} - \frac{iW_V}{1+e^{X_I}} - \frac{4iW_S e^{X_I}}{(1+e^{X_I})^2} - \left(\frac{\hbar}{m_\pi c}\right)^2 \frac{1}{r a_{\rm so}} \frac{(V_{\rm so}+iW_{\rm so})e^{X_{\rm so}}}{(1+e^{X_{\rm so}})^2} \mathbf{l}\cdot\sigma - (-1)^l \frac{V_{\rm ex}}{1+e^{X_{\rm ex}}} + V_{\rm Coulomb}, \quad (4)$$

where $X_i = (r - r_i A^{1/3})/a_i$ and $V_{\rm Coulomb}$ is the Coulomb potential of a uniformly charged sphere of radius $r_c A^{1/3}$.

Optical model parameter sets for the distorted waves and bound state wave function were taken from references cited in Ref. [3] and are listed in Table II. Note that since our calculations were not restricted to a factorized DWIA formalism, spin-orbit terms were included in the distorted waves.

The optical model parameters for the two-body proton-cluster system were obtained by adjusting the set of Comparat *et al.* [12] to give best agreement with experimental free $p + {}^4$He elastic scattering cross section distributions as well as analyzing power angular distributions at an incident energy of 100 MeV. Of course, this causes some deterioration in the optical model agreement with the cross section angular distribution, which was the only type of data used by Comparat *et al.* [12] to determine potential parameters.

The quantum numbers for the bound state wave function were chosen on the basis of conservation of harmonic oscillator shell quanta in the transformation from independent-particle to cluster-model wave functions [4]. This yields

$$2(N-1) + L = \sum_{i=1}^{4} 2(n_i - 1) + \ell_i, \quad (5)$$

where n_i is the principal quantum number and ℓ_i is the orbital angular momentum of each constituent nucleon in the cluster. Therefore, a principal quantum number $N = 3$ and an orbital angular momentum $L = 0$ are found for the bound cluster. The cluster is assumed to be without internal excitation, which is a reasonable assumption, as discussed by Carey *et al.* [4].

IV. ANALYSIS OF DATA

A. Energy-sharing cross section and analyzing power distributions

The measured cross section and analyzing power distributions for the ^{12}C$(p, p\alpha)^8$Be knockout reaction to the ground state are shown in Figs. 2 and 3 for nine quasifree angle pairs. The error bars on each data point represent statistical uncertainties only. Results for the largest proton angle $\theta_p = 110^\circ$ are not shown in Figs. 2 and 3 for space reasons and because they are very similar to the set at $\theta_p = 100^\circ$.

Most of the cross section distributions show a maximum around the quasifree peak, where the residual nucleus has zero recoil momentum as expected. In addition, as was discussed earlier, from $\theta_p = 70^\circ$ to $\theta_p = 110^\circ$, contributions that are probably due to sequential α-particle emission after target excitation can be seen at higher proton energies.

Results of DWIA calculations, performed with the distorting potentials of sets labeled I in Table II, are also shown in Figs. 2 and 3. The DWIA theory reproduces the experimental

TABLE II. Optical potential parameters. All optical potential depths are in MeV and and all lengths are in fm.

System	Set	V_R	r_R	a_R	r_c	W_V	W_S	r_I	a_I	$V_{\rm so}$	$W_{\rm so}$	$r_{\rm so}$	$a_{\rm so}$	$V_{\rm ex}$	$r_{\rm ex}$	$a_{\rm ex}$	Ref.
	I	21.2	1.33	0.65	1.33	6.5	0.0	1.46	0.44	3.86	0.0	0.85	0.43				[13]
$p + {}^{12}$C	II	22.6	1.25	0.55	1.33	4.4	0.0	1.91	0.21	4.30	0.0	0.96	0.49				[13]
	III	21.6	1.30	0.51	1.33	0.0	5.4	1.40	0.52	3.30	0.0	0.97	0.40				[13]
	I	32.3	1.26	0.63	1.30	0.0	2.3	1.31	0.96	4.90	0.0	1.20	0.56				[14]
$p + {}^{8}$Be	II	38.3	1.18	0.62	1.30	3.6	1.0	1.69	0.96	5.60	0.0	1.10	0.58				[14]
	III	38.3	1.20	0.61	1.30	4.8	0.0	1.79	0.66	4.90	0.0	1.12	0.56				[14]
	I	88.9	0.99	0.81	1.20	4.9	0.0	3.01	0.58								[15]
^{4}He $+ {}^{8}$Be	II	94.6	0.97	0.73	1.20	3.05	2.3	2.9	0.48								[15]
	III	65.9	1.48	0.65	1.20	34.9	0.0	1.06	1.05								[15]
$p + {}^4$He		16.3	1.53	0.5	1.36	4.5	4.0	1.7	0.30	10.5	−2.4	0.88	0.26	−10.24	0.13	0.7	[This work]
Bound state		89.9	1.23	0.75	1.23												[3]

energy-sharing distributions reasonably well, except at proton energies below approximately 40 MeV. If one compares our cross section results at $\theta_p = 90^\circ$ directly with those of Chant and Roos [2] at the same angle pair, we certainly find inferior agreement of the theoretical distribution with the experimental values at the lower proton emission energies. The reason for this is clearly that whereas Chant and Roos employ experimental p-^{4}He cross section values in a factorized DWIA, we in effect calculate values with an optical potential that is optimized for an incident energy of 100 MeV. Contrasting our results at this specific angle pair with the work in Ref. [2] suggests that we should keep in mind this limitation in the present analysis at lower proton emission energies. We have chosen not to introduce energy-dependent p-^{4}He optical model parameters but rather to keep input quantities to a minimum to explore the validity of the DWIA in its simplest calculational implementation. Nevertheless, we find encouraging agreement in cross section as well as analyzing power at $\theta_p = 60^\circ$–90°. As we will see later, at zero recoil momentum of the residual nucleus, the trends of the cross section and analyzing power distributions are in remarkable agreement with the DWIA predictions over the full range of proton emission angles covered in this work.

The good agreement between the first three experimental analyzing power values (at $\theta_p = 25^\circ$, 30°, and 37°) and the DWIA predictions in Fig. 5 would seem to be fortuitous if we take into account the poor agreement shown in Fig. 3. However, we should keep in mind that the latter figure offers a very sensitive display, and it draws attention to a proton energy range far from zero recoil momentum where the cross section distribution is also poorly reproduced by the DWIA. Consequently the fact that these experimental knockout analyzing powers are in agreement with those from free scattering should rather be trusted as an indication that the agreement with the theory at zero recoil momentum is probably not accidental.

B. Extraction of spectroscopic factors S_α

The spectroscopic factors are extracted by normalizing the DWIA calculations to the experimental data. The values of spectroscopic factors corresponding to the ten quasifree angle pairs as well as the average value are listed in Table III. Large variations are found in the extracted spectroscopic factors for different angle pairs, but there is no systematic trend. We assign an estimated error to the average value by calculating a standard deviation. Note that the average spectroscopic value is consistent with both the shell model prediction [18] and the average value extracted by Roos *et al.* [3] for the same type of experiment.

TABLE III. Spectroscopic factors for quasifree angle pairs extracted from the data. $\langle S_\alpha \rangle^{\rm exp}$ is a statistical average of all angles.

θ_p/θ_α (deg)	S_α	$\langle S_\alpha \rangle^{\rm exp}$	$S_\alpha^{\rm theory}$ (Ref. [18])
25/−68.8	0.59		
30/−66.6	0.93		
37/−63.1	0.65		
52/55.1	0.19		
60/−50.9	0.20	0.73 ± 0.49	0.56
70/−45.6	0.55		
80/−40.5	0.98		
90/−35.7	1.28		
100/−31.0	1.68		
110/−26.6	0.28		

C. Test of DWIA factorization approximation

In DWIA calculations, when spin-orbit terms are excluded in the distorting potentials, the triple differential cross section may be written in the factorized form

$$\frac{d^3\sigma}{d\Omega_p\, d\Omega_\alpha\, dE_p} = F_K S_\alpha \left\{ \sum_\Lambda \left| T_{BA}^{\alpha L \Lambda} \right|^2 \right\} \left. \frac{d\sigma}{d\Omega} \right|_{p\text{-}\alpha}, \quad (6)$$

where F_K is a kinematic factor, S_α is a spectroscopic factor for the α cluster, and $\frac{d\sigma}{d\Omega}|_{p-\alpha}$ is a half-shell two-body cross section for p-α scattering. The quantity $\sum_\Lambda |T_{BA}^{\alpha L \Lambda}|^2$ is a distorted momentum distribution for an α cluster in the target ^{12}C.

It is thus appropriate to construct the quantity

$$\left[\frac{d^3\sigma}{d\Omega_p\, d\Omega_\alpha\, dE_p} \right]_{\rm exp} \Bigg/ F_K \left\{ \sum_\Lambda \left| T_{BA}^{\alpha L \Lambda} \right|^2 \right\} = S_\alpha \left. \frac{d\sigma}{d\Omega} \right|_{p\text{-}\alpha}, \quad (7)$$

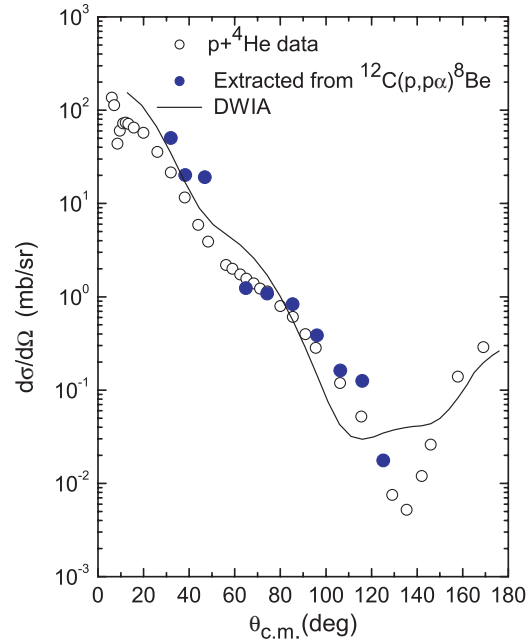

FIG. 4. (Color online) Two-body cross section values (filled circles) as a function of the center-of-mass scattering angle extracted from the experimental $^{12}C(p,p\alpha)^8$Be(g.s.) cross sections at the quasifree peak (zero recoil momentum), compared with predictions of a factorized DWIA theory (curve). In both cases, the average spectroscopic factor listed in Table III was used. For comparison, free elastic scattering data for p-^{4}He at an incident energy of 100 MeV [16] are also shown (open circles).

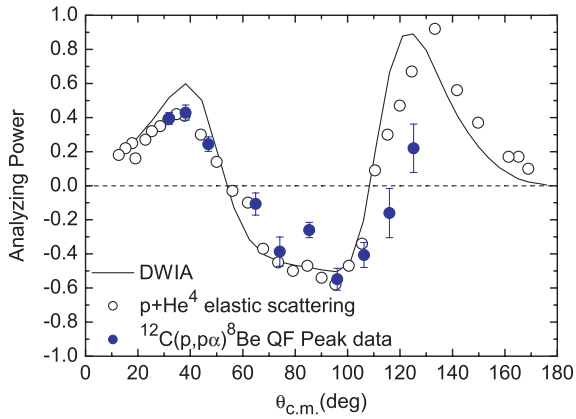

FIG. 5. (Color online) Analyzing power distribution for the $^{12}C(p,p\alpha)^{8}Be$(g.s.) reaction displayed as a function of the two-body center-of-mass p-α scattering angle. Experimental values at the quasifree peak are represented by filled circles with statistical error bars, and the solid curve corresponds to the result of an unfactorized DWIA calculation. For comparison, open circles represent free p-^{4}He experimental analyzing power values at an incident energy of 100 MeV [17].

where $[\frac{d^3\sigma}{d\Omega_p d\Omega_\alpha dE_p}]_{\rm exp}$ now represents the $^{12}C(p,p\alpha)^{8}Be$ experimental cross section value. At the quasifree peak at which zero recoil momentum is kinematically allowed, the quantity on the left-hand side of Eq. (7) is therefore expected to be proportional to the free two-body p-^{4}He cross section.

This comparison is made in Fig. 4. The solid line represents the two-body p-α cross sections $\frac{d\sigma}{d\Omega}(\theta_{\rm c.m.})|_{p-\alpha}$as a function of the scattering angle in the center-of-mass $\theta_{\rm c.m.}$ obtained with DWIA calculations as defined in Eq. (6). The filled circles represent p-α-cluster cross sections extracted from the experimental $^{12}C(p,p\alpha)^{8}Be$ data, corrected for distortion effects (from DWIA theory) and normalized by including the average spectroscopic factor from Table III, as prescribed by Eq. (7). Finally, measured p-^{4}He elastic scattering cross sections at an incident energy of 100 MeV [16] are shown as open circles in Fig. 4. Overall, the results of this comparison are very good and indicate that the factorization approximation works very well over the whole angular range. This means that spin-orbit effects in the distorting potentials have a negligible effect on the convolution of the DWIA cross section.

A more direct and sensitive test of factorization is to compare the coincident $^{12}C(p,p\alpha)^{8}Be$ experimental analyzing power distribution, as a function of the center-of-mass two-body scattering angle, directly with free scattering. Recall that the DWIA analyzing power for the $^{12}C(p,p\alpha)^{8}Be$ reaction is given by

$$A = \frac{\sigma^{\uparrow} - \sigma^{\downarrow}}{\sigma^{\uparrow} + \sigma^{\downarrow}}, \tag{8}$$

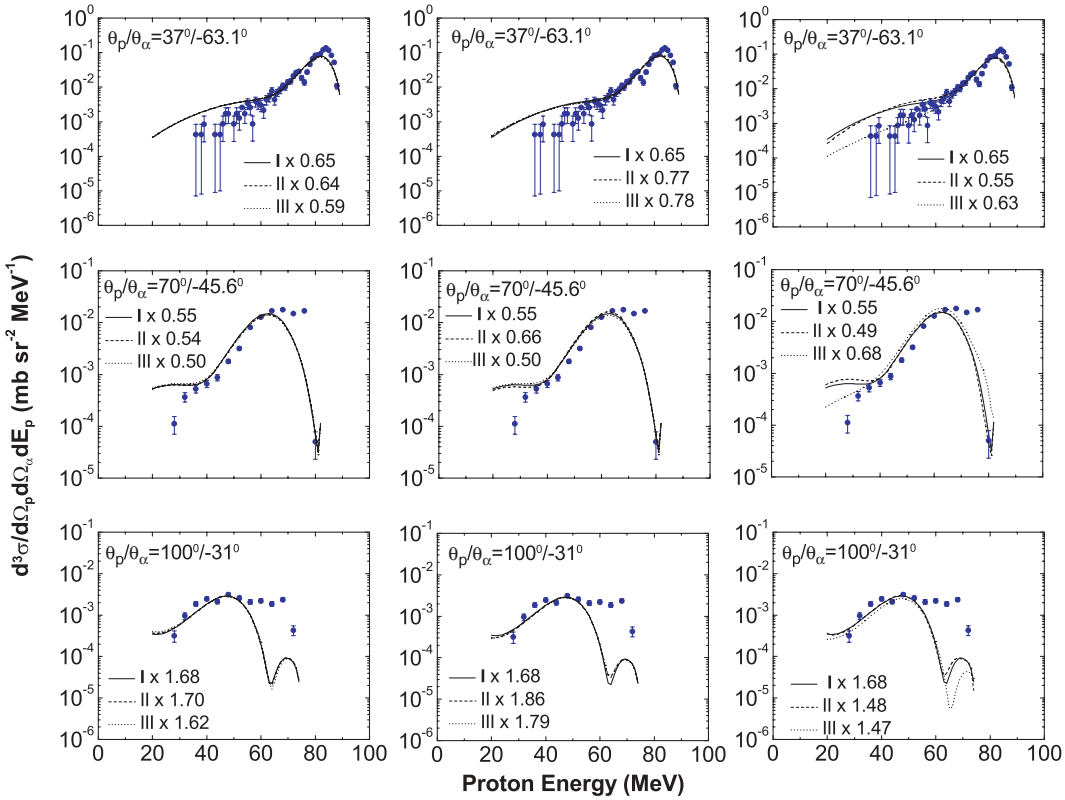

FIG. 6. (Color online) Comparison of energy-sharing cross section distributions with different optical potentials, as listed in Table II. Three optical potential sets I, II, and III are used in the reaction channels $p + {}^{12}C$ (panels left), $p + {}^{8}Be$ (panels center), and ${}^{4}He + {}^{8}Be$ (panels right). Potential identifications are followed by numerical values of the spectroscopic factor for each case.

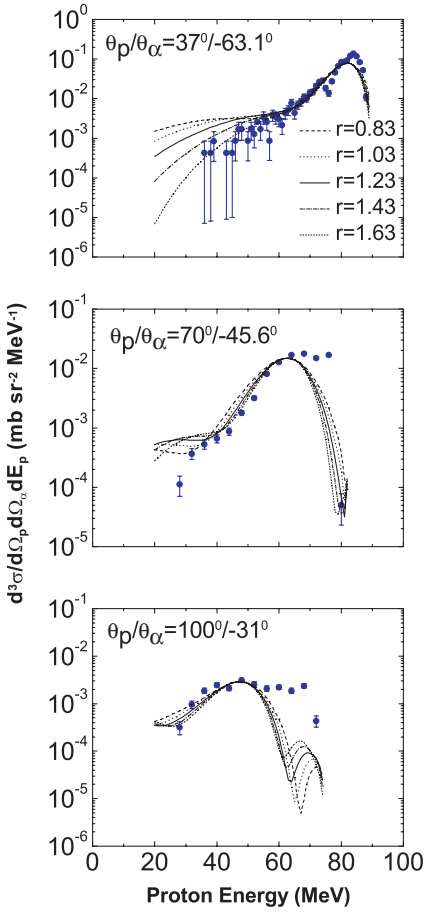

FIG. 7. (Color online) Comparison of energy-sharing cross section distributions with different values of the bound state radius parameter r_R (indicated as r). All curves are normalized to the peak cross section values at zero recoil momentum.

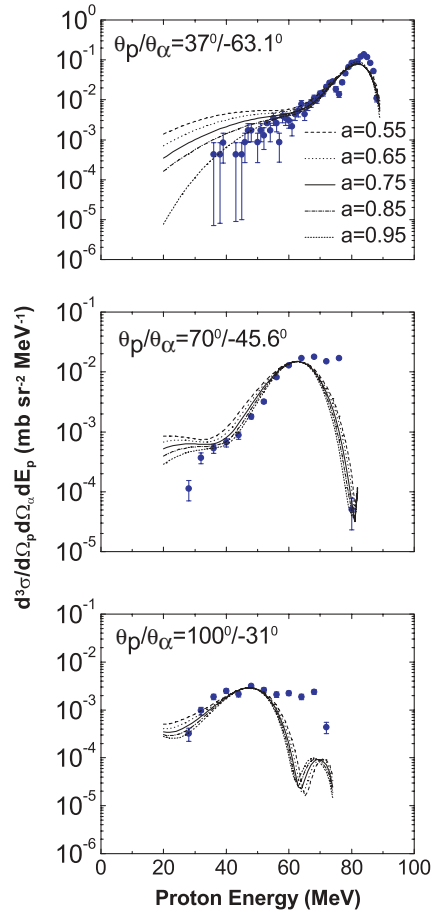

FIG. 8. (Color online) Same as Fig. 7, but for the bound state diffuseness parameter a_R (indicated as a).

where $\sigma^{\uparrow(\downarrow)} \equiv [\frac{d^3\sigma}{d\Omega_p\, d\Omega_\alpha\, dE_p}]^{\uparrow(\downarrow)}$is given by Eq. (2). Therefore, if only the cluster displays a major response to the spin direction of the projectile, the resulting experimental coincidence distribution will approximately factorize and therefore the analyzing power will resemble free scattering. In Fig. 5, this is shown to be true to a remarkable extent. Furthermore, the full DWIA theory, i.e., without the factorization approximation explicitly introduced, reproduces the experimental angular distribution of the analyzing power for the ^{12}C$(p, p\alpha)^8$Be reaction.

D. Sensitivity to distorting potentials and bound state wave function

To investigate the influence of the optical model potential parameters used to generate distorted waves on the values of the coincident cross section, we have chosen three sets for each system. These sets, labeled I, II, and III for each of the systems $p + {}^{12}$C, $p + {}^{8}$Be, and ^{4}He $+ {}^{8}$Be, are listed in Table II. These potential sets are different but roughly equivalent in their descriptions of the appropriate elastic scattering for each particle-target system. Representative results are shown in Fig. 6 for three angle pairs, with the optional parameter sets identified. Each energy-sharing cross section distribution is normalized independently of the experimental values. This implies a dependence of the spectroscopic factor extracted from the experimental data on the exact optical model parameter set. The values indicated in Fig. 6 show this parameter-set dependence to be modest. Furthermore, the shapes of the cross section distributions are almost independent of which specific set is used.

The sensitivity of the cross section results to the radius r_R and diffuseness a_R parameters of the bound state has also been investigated. We confirm the general trend of the results found

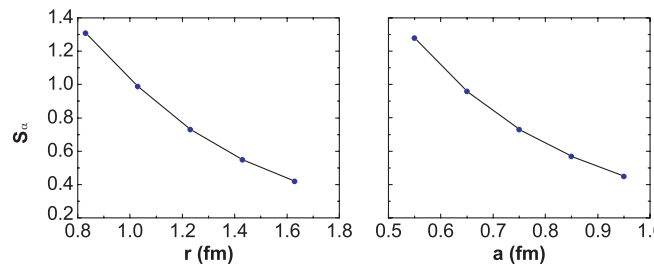

FIG. 9. (Color online) Dependence of the average extracted spectroscopic factor S_α as a function of bound state radius r_R (indicated as r) and diffuseness parameters a_R (indicated as a).

by Carey *et al.* [4] and Roos *et al.* [3]. As shown in Figs. 7 and 8, changes in shape of the energy-sharing cross section distributions are associated with variation in either of the parameter values. Comparison between theoretical prediction and experimental cross section distributions, especially the set for the smallest proton angle, suggests that a slightly larger value of r_R or a_R could be appropriate. However, such an adjustment changes the extracted spectroscopic factor by approximately 40%, as may be inferred from Fig. 9. This variation should be compared with the standard deviation of approximately 70% in the average value of the spectroscopic factor listed in Table III.

V. SUMMARY AND CONCLUSION

The $(p, p\alpha)$ reaction on ^{12}C has been investigated using polarized protons at an incident energy of 100 MeV. Coincident cross section and analyzing power energy-sharing distributions were obtained at ten quasifree angle pairs for proton angles ranging from 25° to 110°. The data were interpreted in terms of a distorted-wave impulse approximation (DWIA) theory. Since measurements of analyzing powers were made, it was appropriate to include spin-orbit distortions in the DWIA calculations. The theoretical distributions reproduce the data reasonably well, which indicates that a quasifree knockout mechanism dominates the reaction. The effects of the spin-orbit interactions in the distorted waves were found to be small, especially near zero recoil momentum. Thus the factorization approximation, where the two-body p-α cross section enters as a multiplicative factor in the three-body $(p, p\alpha)$ cross section expression, is valid. Despite showing a somewhat large spread as a function of angle, the spectroscopic factors extracted from the data were found to be reasonably consistent with theoretical predictions. The analyzing power data at the quasifree kinematic condition follow the trend of free p-^{4}He scattering data remarkably well, and comparisons with DWIA predictions are also in good agreement. These results imply the existence of preformed α clusters in ^{12}C, with a two-body interaction response between the projectile and the α cluster that resembles the scattering of protons from a free α particle to a remarkable extent.

Although the signature of the reaction mechanism is already well established in the present analysis, the theoretical implementation could clearly be refined with respect to calculational sophistication.

ACKNOWLEDGMENTS

We are indebted to the operators and staff of the accelerator group at iThemba Laboratory for Accelerator Based Sciences for providing a stable polarized beam during the experimental work. This work was performed with financial support from the South African National Research Foundation (NRF).

[1] N. S. Chant and P. G. Roos, Phys. Rev. C **15**, 57 (1977).
[2] N. S. Chant and P. G. Roos, Phys. Rev. C **27**, 1060 (1983).
[3] P. G. Roos, N. S. Chant, A. A. Cowley, D. A. Goldberg, H. D. Holmgren, and R. Woody, Phys. Rev. C **15**, 69 (1977).
[4] T. A. Carey, P. G. Roos, N. S. Chant, A. Nadasen, and H. L. Chen, Phys. Rev. C **29**, 1273 (1984).
[5] C. W. Wang, P. G. Roos, N. S. Chant, G. Ciangaru, F. Khazaie, D. J. Mack, A. Nadasen, S. J. Mills, R. E. Warner, E. Norbeck *et al.*, Phys. Rev. C **31**, 1662 (1985).
[6] T. Yoshimura, A. Okihana, R. E. Warner, N. S. Chant, P. G. Roos, C. Samanta, S. Kakigi, N. Koori, M. Fujiwara, N. Matsuoka *et al.*, Nucl. Phys. **A641**, 3 (1998).
[7] R. Neveling, A. A. Cowley, E. Z. Buthelezi, S. V. Förtsch, H. Fujita, G. C. Hillhouse, J. J. Lawrie, G. F. Steyn, F. D. Smit, S. M. Wyngaardt *et al.*, Phys. Rev. C **77**, 037601 (2008).
[8] G. F. Steyn, S. V. Förtsch, A. A. Cowley, J. J. Lawrie, G. J. Arendse, G. C. Hillhouse, J. V. Pilcher, F. D. Smit, and R. Neveling, Phys. Rev. C **59**, 2097 (1999).
[9] A. A. Cowley, P. G. Roos, N. S. Chant, R. Woody, H. D. Holmgren, and D. A. Goldberg, Phys. Rev. C **15**, 1650 (1977).
[10] A. A. Cowley, J. Mabiala, E. Z. Buthelezi, S. V. Förtsch, R. Neveling, F. D. Smit, G. F. Steyn, and J. J. van Zyl, Europhys. Lett. **85**, 22001 (2009).
[11] N. S. Chant, computer code THREEDEE, University of Maryland (unpublished).
[12] V. Comparat, R. Frascaria, N. Fujiwara, N. Marty, M. Morlet, P. G. Roos, and A. Willis, Phys. Rev. C **12**, 251 (1975).
[13] T. Y. Li and S. K. Mark, Can. J. Phys. **46**, 2645 (1968).
[14] G. S. Mani, D. Jacques, and A. D. B. Dix, Nucl. Phys. **A165**, 145 (1971).
[15] R. M. DeVries, J. L. Perrenoud, I. Slaus, and J. W. Sunier, Nucl. Phys. **A178**, 424 (1972).
[16] N. P. Goldstein, A. Held, and D. G. Stairs, Can. J. Phys. **48**, 2629 (1970).
[17] A. Nadasen, P. G. Roos, D. Mack, G. Ciangaru, L. Rees, P. Schwandt, K. Kwiatkowski, R. E. Warner, and A. A. Cowley, Indiana University Cyclotron Facility, Scientific and Technical Report, 1983, p. 13 (unpublished).
[18] D. Kurath, Phys. Rev. C **7**, 1390 (1973).